

RESEARCH

Open Access



# Identification and prediction of developmental enhancers in sea urchin embryos

César Arenas-Mena<sup>1,2\*</sup>, Sofija Miljovska<sup>3</sup>, Edward J. Rice<sup>4</sup>, Justin Gurges<sup>1</sup>, Tanvi Shashikant<sup>5</sup>, Zihe Wang<sup>1</sup>, Sevinç Ercan<sup>6,3</sup> and Charles G. Danko<sup>7,4</sup>

## Abstract

**Background:** The transcription of developmental regulatory genes is often controlled by multiple cis-regulatory elements. The identification and functional characterization of distal regulatory elements remains challenging, even in tractable model organisms like sea urchins.

**Results:** We evaluate the use of chromatin accessibility, transcription and RNA Polymerase II for their ability to predict enhancer activity of genomic regions in sea urchin embryos. ATAC-seq, PRO-seq, and Pol II ChIP-seq from early and late blastula embryos are manually contrasted with experimental *cis*-regulatory analyses available in sea urchin embryos, with particular attention to common developmental regulatory elements known to have enhancer and silencer functions differentially deployed among embryonic territories. Using the three functional genomic data types, machine learning models are trained and tested to classify and quantitatively predict the enhancer activity of several hundred genomic regions previously validated with reporter constructs in vivo.

**Conclusions:** Overall, chromatin accessibility and transcription have substantial power for predicting enhancer activity. For promoter-overlapping cis-regulatory elements in particular, the distribution of Pol II is the best predictor of enhancer activity in blastula embryos. Furthermore, ATAC- and PRO-seq predictive value is stage dependent for the promoter-overlapping subset. This suggests that the sequence of regulatory mechanisms leading to transcriptional activation have distinct relevance at different levels of the developmental gene regulatory hierarchy deployed during embryogenesis.

**Keywords:** Cis-regulatory element, Enhancer prediction, Developmental gene regulation

## Background

Transcriptional regulatory elements (TREs) [1] are the primary drivers of differential gene expression during metazoan development [2–4]. Whereas promoters are TREs easily found by association with the transcription start sites (TSSs) of genes, the identification and

functional characterization of TREs distal to TSSs (enhancers and silencers) remains challenging. Traditionally, enhancers have been considered the modulators of distal transcription at core promoters (promoters thereafter), which integrate inputs from enhancers and ‘proximal promoters’ to initiate local transcription [5]. However, this exclusive functional distinction has been blurred by recent evidence that reveals local transcription initiation at enhancers and promoters that modulate the transcription of some other promoters [1, 2, 5]. Nevertheless, distinct sequences and chromatin features

\* Correspondence: [cesar.arenasmena@csi.cuny.edu](mailto:cesar.arenasmena@csi.cuny.edu)

<sup>1</sup>College of Staten Island, The City University of New York (CUNY), Staten Island, NY 10314, USA

<sup>2</sup>Programs in Biology and Biochemistry, The Graduate Center, CUNY, New York, NY 10016, USA

Full list of author information is available at the end of the article



© The Author(s). 2021 **Open Access** This article is licensed under a Creative Commons Attribution 4.0 International License, which permits use, sharing, adaptation, distribution and reproduction in any medium or format, as long as you give appropriate credit to the original author(s) and the source, provide a link to the Creative Commons licence, and indicate if changes were made. The images or other third party material in this article are included in the article's Creative Commons licence, unless indicated otherwise in a credit line to the material. If material is not included in the article's Creative Commons licence and your intended use is not permitted by statutory regulation or exceeds the permitted use, you will need to obtain permission directly from the copyright holder. To view a copy of this licence, visit <http://creativecommons.org/licenses/by/4.0/>. The Creative Commons Public Domain Dedication waiver (<http://creativecommons.org/publicdomain/zero/1.0/>) applies to the data made available in this article, unless otherwise stated in a credit line to the data.

associate with the prevalence of enhancer and promoter activities among TREs [6]. The expression of inducible genes in unicellular organisms is oftentimes driven by regulatory sequences proximal to the core promoter [2, 5]. In contrast, the oftentimes complex expression of developmental regulatory genes (that is, transcription and signaling factors) is primarily controlled by distal regulatory elements [2, 7]. Despite their relevance, only a few *cis*-regulatory modules (CRMs) that constitute the essential transcriptional nodes of developmental gene regulatory networks are functionally understood [8]. Various high-throughput reporter assay with particular advantages and limitations [9] allow genome-wide testing of enhancer activity [10], and, despite recent progress, most TREs remain largely uncharted [6, 11]. Histone marks such as H3K27ac [12, 13], chromatin accessibility [14] or transcription initiation [15] facilitate the identification of active enhancers. However, the systematic evaluation of the predictive power and redundancy of these genomic marks remains limited [13, 16]. Enhancer transcription may facilitate enhancer activity prediction because it represents the end product, possibly subsequent in most cases to chromatin accessibility set in part by H3K27 acetylation, and because it correlates between enhancers and their target promoters [17–19]. In particular, we are interested in the predictive value of enhancer transcription estimated by the analysis of the transcription run-on assay PRO-seq [20], which detects the differential location of paused and elongating RNA Pol II associated with distinct transcriptional regulatory states [17].

Several experimental advantages have facilitated the exhaustive reconstruction of developmental gene regulatory networks (GRNs) in sea urchin embryos [21–23]. The analysis of topological GRN models reveals an uneven distribution of regulatory sub-circuit motifs along the GRN hierarchy sequentially deployed during sea urchin embryogenesis [4]. Accordingly, the structure and Boolean logic of the TREs serving the nodes of these sub-circuits changes during development too [22]. In sea urchins, enhancer and silencer activities of TREs can be tested by lack of function in bacterial artificial chromosome (BAC) reporter constructs microinjected into zygotes [24, 25], or by gain of function in much smaller plasmid reporters, which oftentimes use heterologous promoters [26]. These exogenous reporters replicate along with the genome [27, 28], with the much larger than plasmids BACs providing a closer approximation to the natural genomic context and more faithfully reproducing the endogenous expression. In addition, BACs maintain endogenous promoters in the context of gene-reporter translational fusions. Despite these advantages, the identification and testing of developmental TREs remains challenging due to the low throughput of existing experimental approaches.

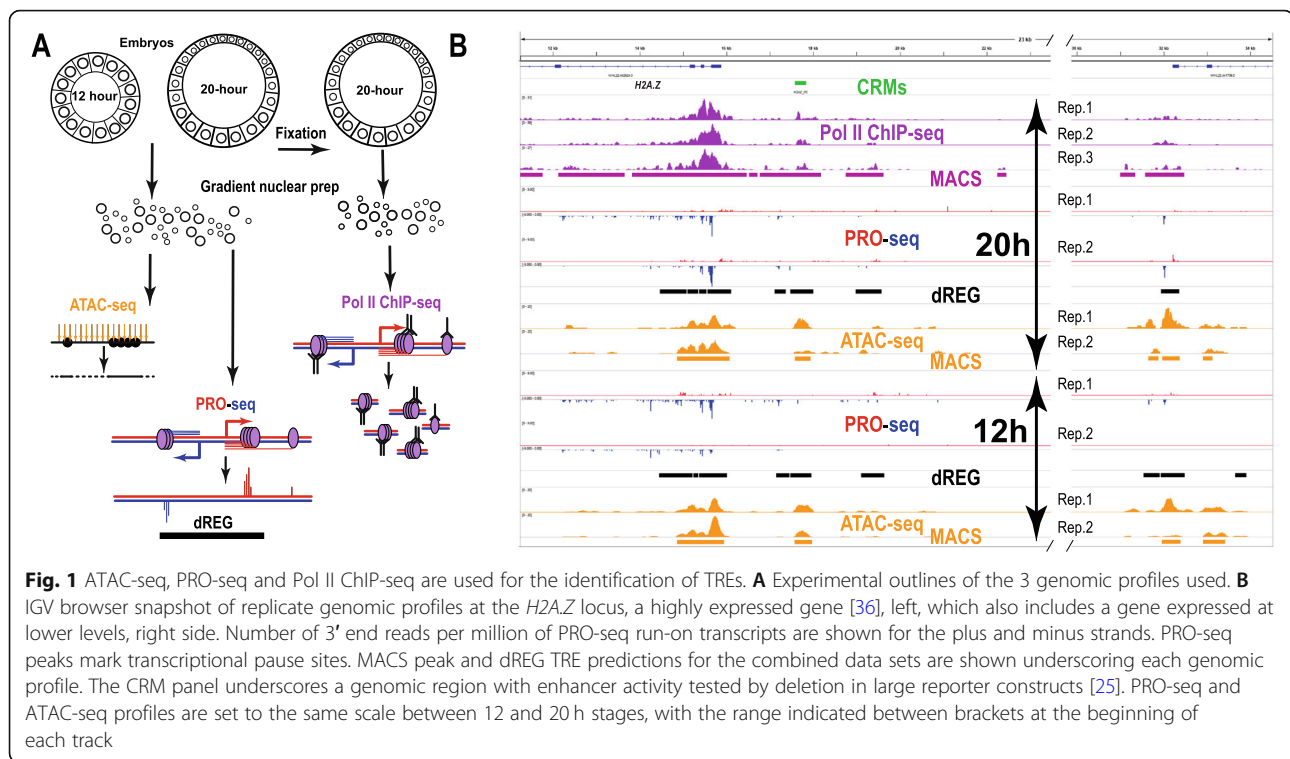
Evolutionary sequence conservation has been routinely used for the identification of potential TREs in sea urchins [4], although conservation is not informative about the stage of regulatory activity, and the obscure cause of diverse evolutionary rates for regulatory sequences [29, 30] raises great uncertainty regarding false positive and negative rates. As in other model systems, chromatin accessibility also facilitates the identification of candidate enhancers in sea urchin embryos [25, 31]. In addition, a parallel reporter method enabled the enhancer activity test of several hundred CRMs associated with 37 developmental regulatory genes during sea urchin development [32, 33]. We used this functional quantification to train and test machine learning model predictors of developmental enhancer activity from various genomic profiles: chromatin accessibility estimated by ATAC-seq [34], RNA Polymerase II (Pol II) distribution, which has been also associated with active enhancers [35], was detected by ChIP-seq, and transcription initiation by PRO-seq (Fig. 1A). Our analysis reveals that chromatin accessibility and transcription both enable enhancer activity prediction, and that the predictive power of these genomic profiles declines during development for the subset of promoter proximal TREs, suggesting a sequence of regulatory shifts at different levels of the gene regulatory hierarchy that is deployed during development.

## Results

### Genomic distribution of chromatin accessibility, pol II and transcription

Chromatin accessibility, transcription and the distribution of RNA Pol II using ChIP-seq were used for the identification of candidate developmental enhancers in 20 h sea urchin embryos (Fig. 1A), and the best performing predictors, ATAC- and PRO-seq, see later, were also characterized in 12 h embryos. The genomic profile of 3' end transcripts identified by PRO-seq was analyzed with dREG (Fig. 1A), a support vector regression tool trained to identify TREs associated with active chromatin marks using the shape of transcription [15]. In 12 and 20 h embryos, dREG identified 43,912 and 56,753 TRE predictions or “peaks”, respectively, while a total of 238,838 and 258,515 ATAC-seq peaks, respectively, were called by MACS (QC reports in supplementary information). In 20 h embryos, 554,846 Pol II ChIP-seq peaks were called.

The dynamic range of the read distribution at peak calls expands several orders of magnitude for the three functional genomic data types (Fig. 2B and D). The Pearson correlation of total PRO-seq reads at dREG peak calls of biological replicates is higher for 12 h embryos ( $R = 0.88$ ,  $p$ -value  $< 2.2 \times 10^{-16}$ , Spearman = 0.71, Fig. 2A) than for 20 h embryos ( $R = 0.35$ ,  $p$ -value  $< 2.2 \times 10^{-16}$ , Spearman = 0.75, Fig. 2C). Similarly, higher correlation



for ATAC-seq profiles at MACS peak calls is found for 12 h embryos ( $R = 0.91$ ,  $p\text{-value} < 2.2 \times 10^{-16}$ , Spearman = 0.79, Fig. 2A) relative to 20 h embryos ( $R = 0.62$ ,  $p\text{-value} < 2.2 \times 10^{-16}$ , Spearman = 0.46, Fig. 2C). The low correlation of PRO-seq biological replicates may be due in part to inherent batch heterogeneity associated with seasonal and genetic variability in the wild populations from which the embryos were obtained. This natural variation may shift the relative timing of major transcriptional regulatory changes during and prior to the 20 h embryo stage, as previously reported [36, 37], along with the associated histone modification and chromatin accessibility signals (Fig. 2).

Interestingly, there is less variability among Pol II ChIP-seq biological replicates ( $R = 0.96$  to  $0.94$ , with  $p\text{-values} < 2.2 \times 10^{-16}$ , Fig. 2C). Nevertheless, the biological or technical source of the variation among the different marks could not be resolved in this study, because different embryo batches, sometimes from different seasons, were used. In addition, for the 20 h ATAC-seq data, a distinct nuclear extraction protocol for one of the replicates [25] may have contributed to some technical variability. Given these caveats no quantitative genome-wide comparison of the different genomic profiles between stages is performed, but only primarily qualitative comparisons among stages based in peak calls (Fig. 2F and Fig. S1 F). However, despite the higher variability of the PRO-seq and ATAC-seq 20 h data sets, generally similar signal profiles are seen among biological replicates in

both developmental stages, as illustrated at the *H2A.Z* locus [25] (Fig. 1B). Similar reproducibility trends are observed at promoters and CRMs (Fig. S1 A-D), with much higher replicate correlations for the subset of CRMs that are the primary target of this study (CRMs hereafter) (Fig. S1 B and D).

Genome-wide, most dREG peaks overlap Pol II peaks (Fig. 2E), as expected. However, because much of Pol II is found in the body of transcribed genes, the majority of pol II peak calls did not overlap with dREG predictions. About 40% of ATAC-seq peaks do not overlap Pol II peaks, and about 90% of ATAC-seq peaks do not overlap dREG predictions, revealing that a substantial fraction of chromatin-accessible regions do not associate with RNA Pol II or transcription initiation detected using dREG, which depends on local transcription initiation profiles. Similar overlapping trends are observed in the CRMs target of this study, with a much larger fraction of ATAC peaks overlapping Pol II peaks, dREG predictions and both (Fig. S1 E), possibly in association with a transcriptional regulatory enrichment in the CRM data set, which is strongly biased for evolutionary sequence conservation [33].

The distinct peak numbers and particular overlaps among the three genomic assays anticipate distinct contributions and/or the requirement of combinatorial analysis for the prediction of distal TREs. Globally, about 42 and 50% of the 12 and 20 h dREG peaks are stage specific, respectively (Fig. 2F), while 36 and 38% of the 12

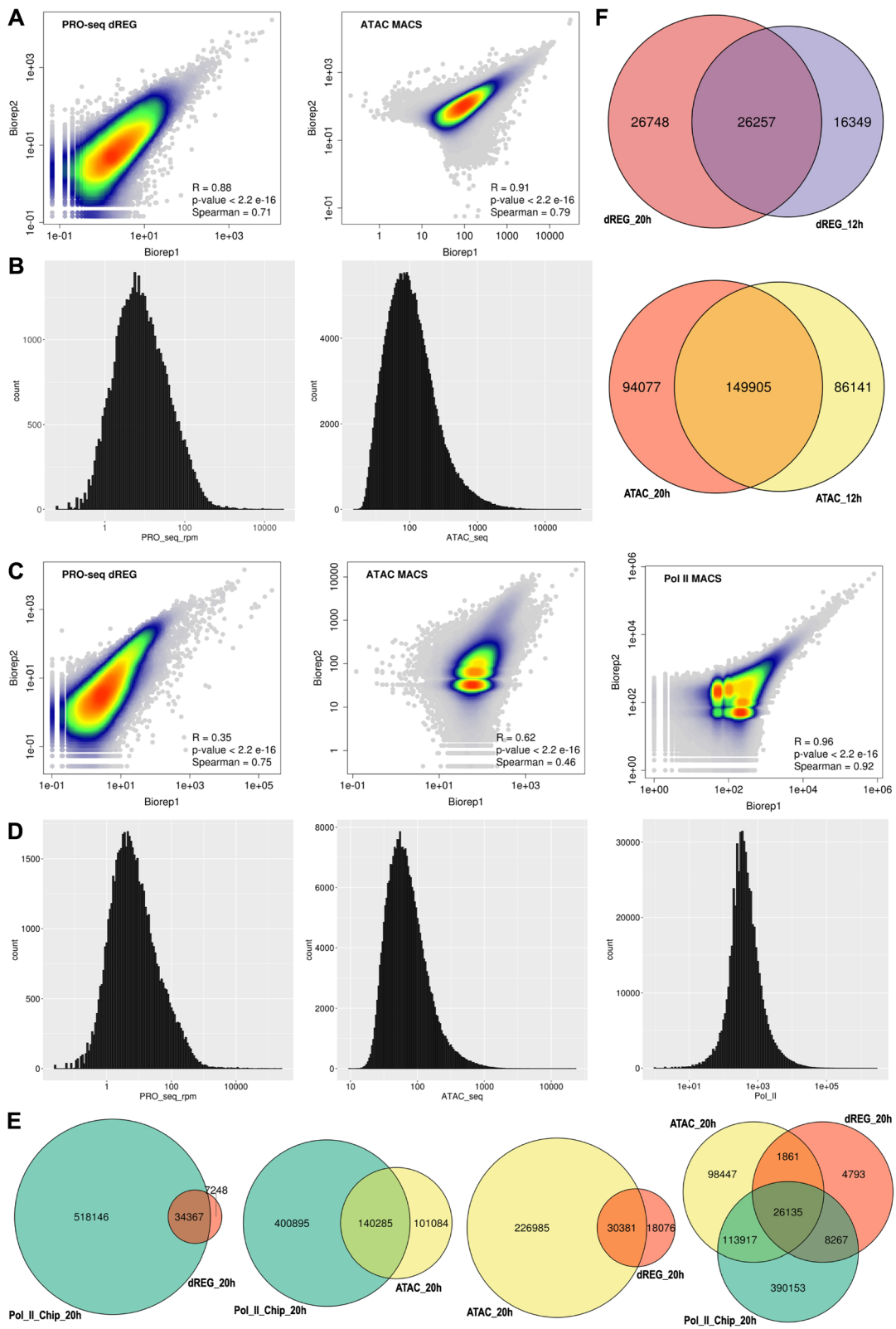


Fig. 2 (See legend on next page.)

(See figure on previous page.)

**Fig. 2** Genome-wide PRO-, ATAC- and ChIP-seq analysis. **A** Distribution of signal intensity and reproducibility estimation between distinct biological replicates for the different data sets in 12 h embryos. Overlap of points indicated by the color gradient. **B** Histograms of the number of reads per peak call for the different data sets in **A**. **C** Distribution of signal and reproducibility in 20 h embryos. **D** Histograms of the number of reads per peak call for the different data sets in **C**. **E** Venn diagrams of the overlap between ATAC and Pol II ChIP peak calls, and dREG predicted TREs in 20 h embryos. **F** Venn diagrams of the overlap of ATAC and dREG peak calls between stages

and 20 h ATAC peaks are stage specific, respectively (Fig. 2F). However, for peaks overlapping CRMs (Fig. S1 F), the majority of ATAC and dREG peaks present in the 12 h stage remain in the 20 h stage, but a much larger proportion of dREG peaks than ATAC peaks are 20 h specific, 60% versus 30%. This reveals that during the 12 to 20 h transition there is a general increase of transcription initiation and pause at developmental TREs while accessibility, estimated by peak calls, is more constant. This suggests that increased accessibility of developmental enhancers generally precedes transcriptional output of developmental TREs.

#### Validation and evaluation of functional genomic marks for the identification of developmental TREs

We manually contrasted our functional genomic data sets with previous experimental *cis*-regulatory analyses in order to explore how they could facilitate the identification of active developmental TREs. TRE necessity for

the control of endomesoderm transcription factor *SpHox11/13b* developmental expression has been characterized by deletion from BAC reporters, and TRE sufficiency by plasmid reporter constructs testing an overlapping array of genomic regions that scan the entire locus [24]. ATAC-seq peaks underscore regulatory element ME in 12 and 20 h embryos but only dREG highlights ME in 20 h embryos (Fig. 3), which corresponds to the stage of higher ME reporter activity [24].

This pattern of 20 h specific dREG activity follows the general ATAC and dREG stage prevalence trend in the proximity of regulatory elements, a generally constant number of ATAC peaks and increased number of dREG peaks during the later blastula stage (Fig. S1 F). Module ME has been demonstrated to be both necessary by deletion in BAC reporters and sufficient in plasmid reporters [24] to drive the embryonic *SpHox11/13b* expression profile, which is spatially dynamic and increases during the 12 to 20 h transition [38]. Like many



**Fig. 3** ATAC-, Pol II ChIP- and PRO-seq sea urchin embryos at the *SpHox11/13b* locus. For ATAC- and PRO-seq, the scale in reads per million at the start of each track is maintained at the same range between states and equal between plus and minus strands. The whole region was scanned for enhancer activity by overlapping 3–5 Kb reporter constructs [24], only active CRMs are indicated, in green those active in both stages, and in gray those inactive or with unknown activity in these stages as indicated in the text

other early embryo TREs, ME has distinct enhancer and silencer functions in different embryonic territories. In 12 and 20 h embryos, module ME responds to spatially restricted vegetal *wnt* signaling by enhancing transcription in the endomesoderm and endoderm territories, and by silencing transcription in the ectoderm and the mesoderm, where the *wnt* pathway remains and becomes inactive, respectively [24]. Therefore, the whole embryo genomic profiles derive from both enhancer and silencer activities from different territories.

DNA binding sites for transcription factor TCF are required for the *wnt* signal dependent enhancer and silencer functions of element ME. There is an increase in the transcriptional pause at the 20 h embryo *SpHox11/13b* promoter relative to the 12 h stage (Fig. 3), which could correspond with its ME transcriptional silencing in the ectoderm and mesoderm [24]. Interestingly, the cofactor of TCF, groucho, implements silencing by pause in *Drosophila* embryos [39], which may represent an evolutionarily conserved function in sea urchins. Module D, in isolation, drives unrestricted reporter expression in 15 and 18 h embryos that can be dominantly silenced by module ME when placed in the same reporter construct [24]. Module D is inactive in 6 and 21 h embryos, leaving uncertain its activity in 12 h embryos. There are ATAC-seq peak calls with relatively low signal within Module D in both stages, but no dREG peaks (Fig. 3). Thus, module D lacks silencing functions and dREG peak calls.

Module D was not deleted in BACs and therefore its endogenous function remains uncertain [24]. Finally, element L, which drives reporter activity at later stages, was undetectable with reporter constructs in 15 and 24 h embryos [24], dREG marks regulatory element L in 20 h embryos but not in 12 h embryos, while ATAC detects this regulatory element in both stages. In this case, the dREG peak calls and associated pausing in module L of 20 h embryo may correspond with its priming for subsequent activation during later embryonic and larval stages.

Similar unbiased tiling array reporter scan was performed for the regulatory elements controlling the expression of transcription factor *onecut* [40]. During pregastrular stages, *onecut* zygotic transcript levels reach a minimum soon after the 12 h stage and peak at 20 h, around the time when its restricted oral-aboral boundary expression is established [40]. Analogous to *SpHox11/13b* module ME, distal regulatory module Intron-D of *onecut* integrates enhancer and silencer functions that are necessary and sufficient to recapitulate the expression of this transcription factor [40]. Likewise, ATAC-seq peak calls underscore Intron-D in both stages, but only 20 h dREG peak calls highlight Intron-D, coincident with an augment of pause at the *onecut* promoter (Fig. S2). Thus, both in *SpHox11/13b* ME and *onecut* Intron-D

PRO-seq signals may correspond to a blend of transcriptional activation and silencing functions in different embryo regions. Only ATAC-seq peaks intersect *onecut* Intron-C module, which is inactive in 20 h embryos (Fig. S2). Thus, similar to module L of *SpHox11/13b*, the ATAC-seq peak call does not correspond with enhancer activity.

There are far more ATAC-seq peak calls than dREG predictions at both loci (Fig. 3 and Fig. S2), along with the general genomic trend (Fig. 2E). Both loci were scanned by a comprehensive reporter tiling scheme to test the entire regions for enhancer activity in an unbiased manner [24, 40]. Remarkably, dREG TRE predictions correspond closely with regulatory elements experimentally mapped to their minimum range (Fig. 3 and Fig. S2). However, most dREG predictions do not match CRM enhancer reporter activity (Fig. 3 and Fig. S2), and even a higher proportion of ATAC peaks do not correspond with enhancer-active CRMs. The distribution of Pol II ChIP peaks is even broader, particularly at introns, which are prone to contain TREs (Fig. 3 and Fig. S2), and, therefore, Pol II ChIP signal seems poorly suited for TRE predictions on its own. Manual analysis of other experimentally characterized transcriptional regulatory elements [41–43] generally confirms the trends outlined above (Fig. S2). Additional regions of the genome can be analyzed with the data sets deposited at the NCBI Gene Expression Omnibus [44], which include ATAC-, Pol II ChIP- and PRO-seq genomic profiles along with their associated peak calls. In summary, our manual analysis suggest that accessibility may have a looser correspondence with enhancer activity. In addition, although increased pause does not necessarily correspond with silencing, as it may be associated with increased release and elongation, the dual report of transcriptional elongation and pause by PRO-seq may correspond to enhancer and silencer activities differentially deployed in space, which is very common among early embryo regional specification TREs [4].

#### Prediction of enhancer activity from chromatin accessibility and pol II

We decided to systematically test if machine learning models using chromatin accessibility, Pol II distribution and transcription initiation could predict the previously quantified enhancer activity of 389 CRMs (Supplementary Table 1) primarily selected for their evolutionarily sequence conservation [33]. We first tested a subset of reporters quantified at high temporal resolution using nanoString technology [32], but the very small number of inactive reporters was unsuitable for model training (results not shown). We therefore settled for a previous data set that measured reporter enhancer activity by qPCR and included 12 and 24 h time points [33].

Although this generated a mismatch with the 20 h stage examined in our genomic data, no major regulatory transitions have been identified for the majority of the genes involved during this 4 h period [45]. The average size of the 389 CRMs (2839 bp) is about one order of magnitude larger than the average of ATAC peaks (316 bp) Pol II peaks (338 bp), and dREG TRE predictions (373 bp) (Fig. 4A). Thus, in order to reduce confounding inputs to the CRMs that may not relate to TRE function, such as background transcription at introns, or background accessibility along the CRM span, the ATAC-, Pol II ChIP- and PRO-seq signals were computed at CRM regions overlapping peak calls and dREG predictions. CRMs were defined as active if they drove reporter expression twice above the basal promoter (Fig. 4B and C). CRM activity cannot be explained by CRM size because there is no significant size difference between active and inactive enhancers (Fig. 4A, inset, Wilcoxon  $p$ -value = 0.11). However, active CRMs in 12 and 24 h embryos have significantly higher PRO-, ATAC-, and Pol II ChIP-seq signals (Fig. 4D,  $p$ -values < 1.8 e-06).

Logistic regression classifiers trained and tested by 5 fold cross-validation repeated 200 times resulted in predictions significantly above random guess in both embryo stages (Fig. 4E and F). The performance of models using ATAC, dREG (PRO-seq reads at TRE dREG predictions), their combination (ATAC + dREG), and Pol II ChIP was slightly higher for ATAC + dREG models when evaluated by the Area Under the Receiver Operating Characteristic (AUROC) plot (Fig. 4E and F), which graphs the relation between true and false positive rates at different model prediction thresholds. However, the CRM expression data set is highly unbalanced, with about 10 times more CRMs reporting inactive than active enhancer activity (Fig. 4B and C), and, in these cases, Precision-Recall Curves (PRCs), which plot precision values along the range of true positive rates, provide a better discrimination metric for classifier evaluation [46].

When AUPRCs are used for model evaluation, more distinct model performances are obtained, particularly for the 20 h data sets (Fig. 4F, bottom). Individually, all assays perform much better than chance in both stages (Fig. 4E and F). The combination of ATAC and dREG predictors barely improves performance at some recall values (Fig. 4E and F, bottom), and similarly, Pol II ChIP signal does not facilitate better enhancer activity predictions alone (Fig. 4F) or in combination with other data sets (results not shown). The limited model improvement with combined data sets is perhaps expected given their substantial correlation, with Pearson's correlation coefficients ranging from 0.6 to 0.8 between predictors of the same stage. Incorporation of other parameters

such as peak summit value, did not improve any predictive models, as illustrated for dREG (Fig. 4H). As expected, lower model performance was also obtained when the functional genomic data were computed along the entire CRM instead of restricting the signal input to peak call windows (not shown). Optimization of other machine learning methods, such as random forest and support vector machine, did not improve classifier performance over logistic regression (not shown), likely reflecting the small size of the available data. In short, total ATAC-seq and PRO-seq signals at dREG peaks are the best predictors of active enhancer activity among the profiles tested in this study.

About half of the CRMs that overlap promoters are active in the reporter assays, indicating a high degree of enhancer activity from promoter-adjacent DNA in sea urchin embryos [33]. Nearly all these promoter-overlapping CRMs were previously shown to be active in both orientations [33], demonstrating bona fide enhancer activity. We further confirmed that the concurrent and divergent orientation of promoter-overlapping CRMs in reporter constructs were evenly represented in our data set and did not correspond with significant enhancer activity differences (Fig. S3), excluding the relevance of confounding effects due to transcription initiation at the CRMs followed by elongation into the reporter. The sizes of promoter-overlapping CRMs (Fig. 4A) suffice to include both distal and proximal TREs, including promoters. Interestingly, ATAC and dREG models trained with the entire data set (Fig. 4F) underperformed relative to Pol II ChIP based models in the prediction of enhancer activity of the promoter-overlapping CRM subset (Fig. 4G, top). In the complementary analysis, the Pol II ChIP model trained with the entire set further underperformed relative to ATAC and dREG models in the prediction of CRMs not overlapping promoters, while ATAC and dREG maintained performance similar to predictions with the entire set (Fig. 4G, bottom). The exclusion of the 41 promoter-overlapping CRMs from the training and testing data set decreased the prediction performance of all models in both stages (Fig. S4 A and B). Overall performance was broadly similar between ATAC and dREG models trained and tested with the promoter overlapping or non-overlapping in 12 h embryos (Fig. S4 A and C). In contrast, ATAC and dREG models trained with CRM-overlapping promoters failed to predict the activity of their hold out set and were outperformed by Pol II ChIP models in the 20 h data set (Fig. S4 D). All of the above, reveals that the enhancer activity predictive power of ATAC-seq and PRO-seq for promoter-proximal CRMs dramatically devalues during the 12 to 20 h transition.

The larger proportion of positive enhancers among CRMs that overlap promoters relative to CRMs not

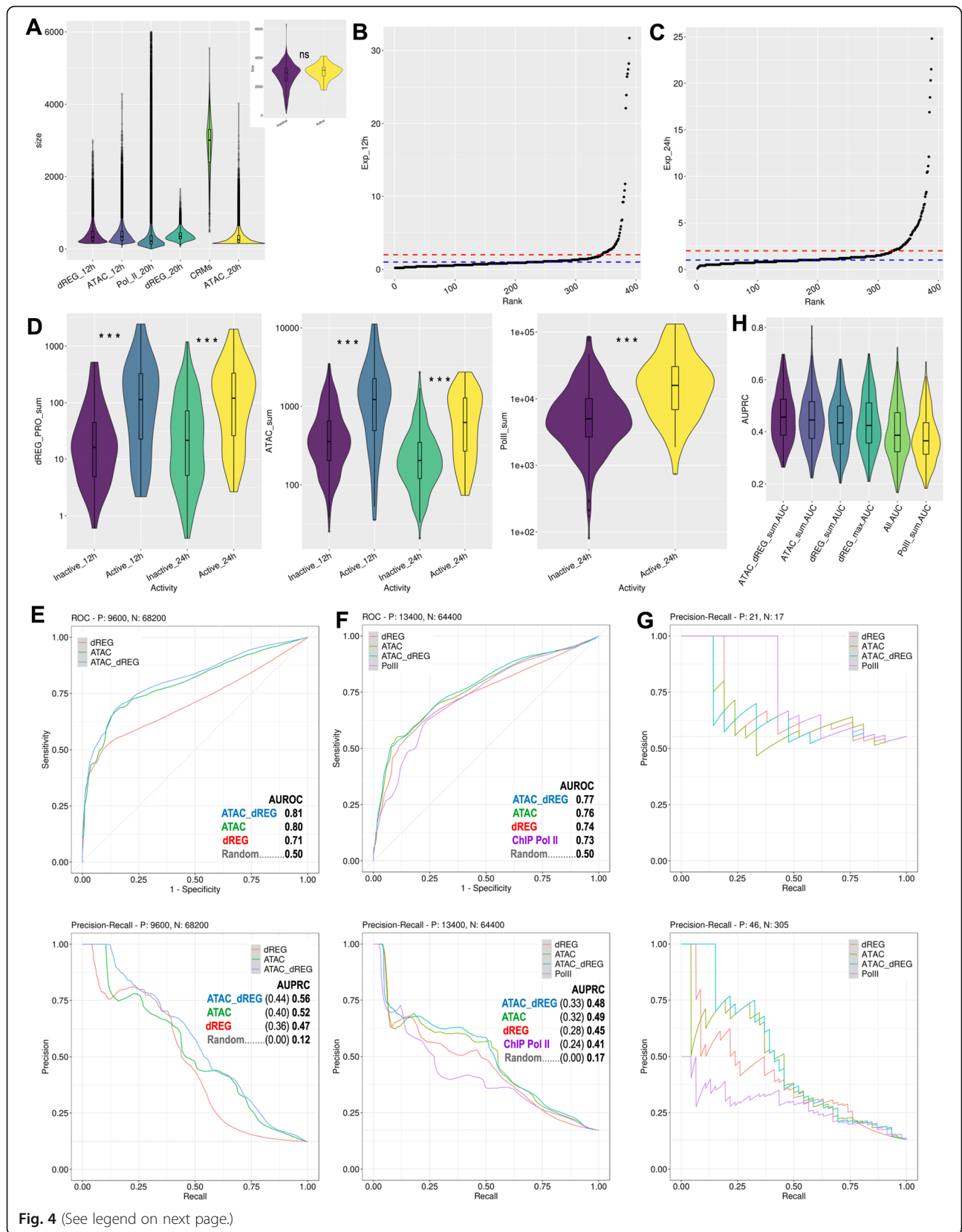


Fig. 4 (See legend on next page.)



(See figure on previous page.)

**Fig. 4** Modeling of CRM reporter activity from ATAC-, Pol II ChIP- and PRO-seq. **A** Violin/box-plot of the ATAC, Pol II ChIP peak call and dREG TRE prediction sizes, and the 389 CRMs. The inset plots the size distributions of active and inactive CRMs, which is not significantly different. **B** and **C**, ranked CRM expression plot in 12 and 24 h embryos, respectively. The blue line at 1 marks the CRM expression level when it equals that of the basal-promoter reporter. The red line by the curve “elbow” marks the 2 fold above control chosen as the expression threshold. **D** Violin/box-plots of PRO-, ATAC-, and Pol II ChIP-seq significantly different signals between active and inactive CRMs in 12 and 20 h embryos. **E**, top, 12 h embryo Receiver Operating Characteristics (ROC) and, bottom, Precision-Recall Curves (PRC) of the logistic regression models trained and tested by 5 fold cross-validation repeated 200 times. Area Under the ROC (AUROC) and AUPRC as indicated for each model. Dotted lines mark random guess prediction performance, a mid-diagonal for ROC and a horizontal line at the fraction of active CRMs for PRC. The absolute AUPRC indicated in bold and the difference with random guess in parenthesis. **F** ROCs and PRCs in 20 h embryos. **G**, top, PRCs evaluating the enhancer activity predictions for the CRM promoter-overlapping data set of models trained with the entire 20 h CRM data set. Bottom, model predictions for the complementary, non-promoter overlapping data set. **H** Violin/box-plot of the AUPRC after cross-validation with different predictors, as indicated; All, includes the sum and max of the 3 genomic profiles allowing second order interactions among predictors; dREG-max, signifies the sum of the maximum values at dREG peaks

overlapping promoters, ~50% vs. ~13% in 20 h embryos, is not surprising given the bias for regulatory genes active during development of this data set [33] combined with the general trend of enhancers to be near their promoter targets [47]. The enhancer activity of promoters has precedents [48, 49] and it is perhaps not surprising for evolutionary reasons [2].

We tested if the functional genomic datasets could predict the levels of reporter enhancer activity of CRMs. In all cases, better linear regression model prediction was obtained with non-promoter overlapping CRM sets. The best performing model included the ATAC-seq plus the ATAC:dREG interaction, which explained about one third of the expression variation (average  $R^2 = 0.29$ ) in 20 h embryos (Fig. 5). ATAC-seq was a better predictor

of enhancer activity in 20 h embryos relative to 12 h embryos ( $R^2 = 0.26$  versus  $R^2 = 0.17$ ,  $p$ -value  $< 2.2 \times 10^{-16}$ ), and outperformed dREG in 20 h embryos ( $R^2 = 0.17$ ,  $p$ -value =  $7.4 \times 10^{-16}$ ) (Fig. S5). The difference in dREG model performances between stages or with ATAC-seq models in 12 h embryos was not significant due to the small size of the dataset. Nevertheless, the relative enhancer predictive power of ATAC-seq and PRO-seq is stage-dependent. The predicted value of most CRMs generally varies with the training set, as expected. However, there is a group of CRMs that are consistently and erroneously predicted as barely active (Fig. S5) due to their low signals in all assays (not shown). Highly active reporter constructs with low predictor signals may result from not uncommon miss-regulation outside the endogenous

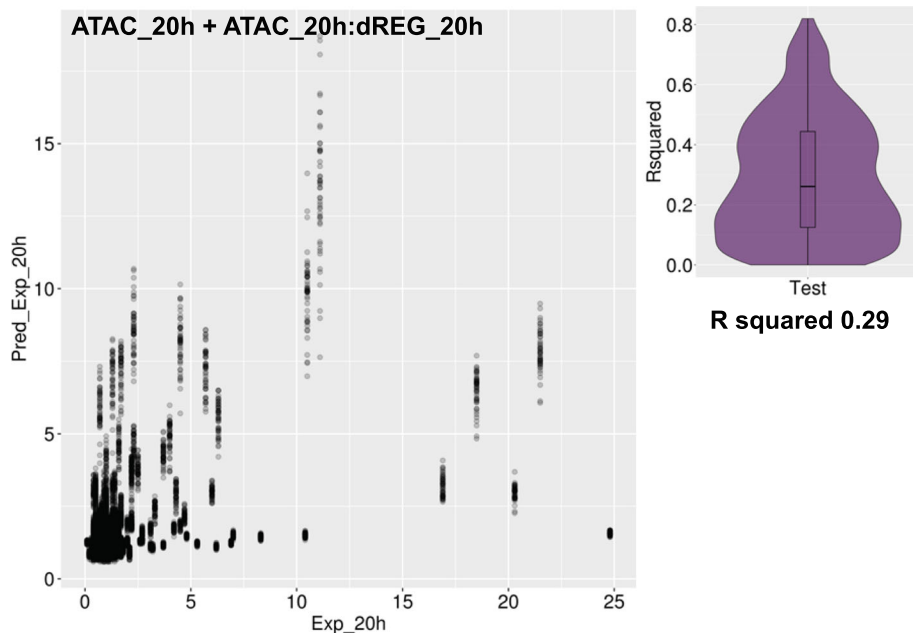


**Fig. 5** Quantitative prediction of enhancer activity from PRO-seq data. Plot of the hold-out predicted against the actual reporter expression of linear regression models using ATAC and PRO-seq signal at dREG predictions tested by five-fold cross-validation. Violin/Box-plot of  $R^2$  values, with the average indicated underneath

genomic context [4], which may cause ectopic expression, such as the one observed for *SpHox11/13b* module D [24], or it may reflect mismatches between the time points, especially at the 20 h stage.

## Discussion

Machine learning models identify ATAC- and PRO-seq as efficient predictors of the developmental enhancer activity of genomic regions previously validated by their reporter driven expression in sea urchin embryos (Fig. 4E and F). Further prediction improvements are expected after addressing some limitations and biases in of our experimental setup. First, the bulk functional genomic profiles of whole embryos represent a blend of several transcriptional states present in different territories. The unavoidable bias against enhancers only active in a few cells should nevertheless correspond with similarly biased CRM reporter expression levels. More problematic could be the confounding enhancer and silencer activities in different territories for the same element, which are common in developmental gene regulation [4, 50], as previously discussed in the context of *SpHox11/13b* and *onecut* (Fig. 3 and Fig. S2). Future single-cell ATAC-seq studies will increase the spatial resolution over whole embryo characterizations, such as the one presented here, which are nevertheless required for validation. To our knowledge, there is no single-cell approach for PRO-seq. However, single-cell resolution should be also developed for the CRM functional assays in order to fully overcome this limitation. Second, the mismatch between the size of TRE peak calls and CRMs tested is less than ideal (Fig. 4A). In most high-throughput reporter assays [10], the regulatory regions tested are usually smaller than the few hundred base pairs of common TREs, which represents one of the several limitations of enhancer activity evaluation by reporter constructs [10]. In contrast, the genomic regions tested in our data set are large (Fig. 4A) and often contain several ATAC and dREG peak calls, whose signals would possibly better match enhancer activity if individually tested. Third, the CRMs functionally tested are biased for evolutionary sequence conservation, which may exclude functional but fast evolving CRMs. Thus targeting the functional analysis to ATAC-seq and dREG peak call regions would be more suitable to analyze the predictive value of these genomic profiles. Fourth, inherent to most high throughput reporter assays, enhancer activity is tested with a heterologous promoter, allowing for the mismatch between functional genomic assays and reporter activity due to enhancer-promoter specificity [51].

Despite the tight match between dREG TRE predictions and CRMs experimentally narrowed down to the smallest functional regulatory elements in a generally unbiased manner (Fig. 3), our results reveal that PRO-seq has similar predictive power as ATAC-seq. Perhaps

this results from the dual report of transcription and pause by PRO-seq. Alternatively, the small set of positive enhancers measured by reporter assays could result in having insufficient statistical power. Nevertheless, despite all these caveats, ATAC-seq and PRO-seq alone suffice to explain between one quarter and one fifth of the reporter enhancer activity in 20 h embryos (Fig. 5 and Fig. S5). It is reasonable to expect even better performance in single cell assays exclusively testing the genomic regions highlighted by ATAC- and PRO-seq profiles.

Our results confirm and extend reports of distinct enhancer prediction performance for promoter-proximal regulatory elements previously obtained with a distinct set of functional genomic profiles [11].

The higher enhancer activity predictive power of Pol II for the promoter-overlapping subset (Fig. 4G and Fig. S4 B and D) is not surprising, because the endogenous Pol II signal due to effective transcription should parallel transcription driven by the promoter of the reporter construct whenever relevant regulatory elements are included in the CRM (Fig. S3 A). Interestingly, ATAC and PRO-seq profiles are irrelevant for the prediction of promoter-overlapping CRMs in 20 h embryos (Fig. 4G and Fig. S4 C and D). The lower predictive power of ATAC and PRO-seq for the promoter overlapping subset may relate to enhancer sharing between the endogenous promoter and the reporter promoter (Fig. S3 A), which should be biased against the reporter promoter due to enhancer-promoter specificity. In other words, the endogenous promoter represents a perfect match and should more effectively sequester any local enhancers included in the CRM, therefore lowering reporter activity. This potentially confounding factor for promoters that are tested for enhancer activity in reporter assays may be difficult to address because the core promoters of enhancers are functional components required for their enhancer activity [18]. More interestingly, different from the 20 h embryos case, ATAC- and PRO-seq profiles have similar predictive power for promoter-overlapping CRMs relative to distal CRMs in 12 h embryos (Fig. S4 C and A). This suggests that distinct transcriptional regulatory mechanisms, including those related to enhancer-promoter specificity, may prevail at TREs used at different levels of the gene regulatory hierarchy that is sequentially deployed during sea urchin development [45], or that regulatory genes are at distinct stages in the sequence of events leading to their transcriptional activation during the 12 to 20 h transition. Alternatively, the potential enhancer-sharing bias against promoter-overlapping CRMs mentioned above may be more pronounced in the 20 h stage, when most of the 37 regulatory genes subject of this study [32] are activated (Fig. S6).

Along with major transcriptome changes during the 12 to 20 h transition [36], the majority of the 37 regulatory genes undergo more than a twofold change in transcript levels (Fig. S6), in agreement with their position in the topological models of the BioTapestry Interactive Network Viewer [45]. In short, the activation of the upstream regulatory genes that determine the main territorial subdivisions is underway in the 12 h blastula, while the transcriptional states determining these subdivisions are well established in the 20 h blastula, including the activation of terminal differentiation gene batteries at the periphery of the transcriptional network [21–23, 45, 52]. In general, more PRO-seq than ATAC-seq associated changes are observed during the 12 to 24 h transition (Fig. S1 F), in agreement with punctual observations (Fig. 3 and Fig. S2). This would follow the general sequence of events in the transcriptional cycle [53], with enhancer accessibility preceding transcriptional initiation, followed by pause and release, all of which are target of regulation by sequence specific transcription factors. The early territorial subdivisions are mediated both by transcriptional enhancer and silencer functions, and the relation of functional genomic profiles to experimental characterizations (Fig. 3 and Fig. S2) suggest that pausing may not only provide a venue for coordinated and prompt transcriptional activation during development [54], but also anticipate permanent silencing in some territories.

## Conclusions

In summary, ATAC- and PRO-seq are efficient predictors of reporter enhancer activity of distal CRMs in sea urchin embryos, while the prediction of promoter-overlapping CRMs is stage-dependent. In late blastula embryos, Pol II enrichment is the best predictor of promoter-proximal CRM enhancer activity. There is a net increase in dREG TRE predictions during later embryonic stages, while accessibility peaks remain relatively constant. In combination, this suggests that the sequence of regulatory events leading to developmental TRE enhancer activity has different relevance at different GRN levels or developmental stages. Our work facilitates ongoing developmental gene regulatory studies by mapping genome-wide candidate TREs, identifies PRO-seq and ATAC-seq as candidate factor-independent methods that predict developmental enhancer activity in whole embryos, and outlines the stage-dependency and predictive value of distinct functional genomic profiles associated with proximal and distal regulatory elements.

## Methods

### Preparation of nuclear extracts and sequencing libraries

Sea urchin embryos were reared to different stages as previously described [25]. Nuclei for ATAC-seq and PRO-seq were prepared using a modified version of a density gradient method [55] as follows. Sea urchin embryos were centrifuged at 500 g for 3 min at 0 °C, the pellet was resuspended in 10 volumes of ice cold lysis buffer consisting of 20 mM EDTA, 2% polyethylene glycol, and 4 mg/ml of Protease Inhibitor Tablets (Thermo Scientific™ Pierce™ #A32965), added just before use, in 0.1 X PBS (PBS is 0.137 mM NaCl, 2.7 mM Cl, 10 mM Na<sub>2</sub>HPO<sub>4</sub> and 18 mM KH<sub>2</sub>PO<sub>4</sub>), and incubated on ice for 5 min. Dissociated cells were further disrupted with 50 or more strokes in a fine dounce homogenizer. Density gradient nuclear wash and floating layers were prepared by diluting iodixanol 60% (OptiPrep™) in 1 X PBS to 20 and 40%, respectively. About 5 ml of nuclear lysate was deposited on top of 10 ml of nuclear wash and nuclei were collected over 200 µl of floating layer after centrifugation for 30 min at 2 °C and 3000 g in a swing bucket rotor. Nuclei aliquots were flash-frozen in liquid nitrogen. For the 20 h stage, nuclei of one of the two ATAC-seq biological replicates was prepared as previously described [25]. For ChIP-seq, fixation was performed by resuspending embryo pellets in crosslinking solution (1 mM EDTA, 0.5 mM EGTA, 100 mM NaCl, 1.8% formaldehyde, 50 mM HEPES, pH 8.0) for 15 min at 22 °C, followed by gravity settling and subsequent resuspension in stop solution (125 mM glycine, 0.1% Triton X-100 in PBS), 500 g centrifugation, and two washes with PBT (0.1% Triton X-100 in PBS). The embryos were transferred to 25 ml of ice cold homogenization buffer (15 mM Tris-HCl pH 7.4, 0.34 M sucrose, 15 mM NaCl, 60 mM KCl, 0.2 mM EDTA, 0.2 mM EGTA, with 4 mg/ml protease inhibitors) and incubated on ice for 5 min. Embryos were first dounced 20 times with pestle type A (loose), followed by 10 times with pestle type B (tight). Nuclei were then filtered through a 20 µm filter and pelleted at 3500 g for 5 min at 4 °C. The nuclei were resuspended in 7.5 ml of PBTB (5% BSA in PBT buffer, with proteinase inhibitors). Propidium iodine stained nuclei were quantified using a hemocytometer and a fluorescence microscope.

ATAC-seq library preparation and Illumina sequencing followed similar procedures to those previously described [34]. The ENCOCE-DCC atac-seq-pipeline [56] was used for mapping the raw reads to the *S. purpuratus* genome version 3.1 using default settings, except for the MACS2 peak call p threshold, which was set to 0.05. Two biological and one technical replicate libraries were paired or single end sequenced. A total of 16,005,927 20-h and 73,272,494 12-h embryo reads mapped to the genome after deduplication and mitochondrial

chromosome filtration. About 44% of the reads locate in peak calls, see quality control summary for detailed reproducibility and sequence quality metrics ([Supplementary quality control files](#)).

PROseq libraries were elaborated following previously established protocols [17], single or paired end sequenced in Illumina platforms, and mapped to the *S. purpuratus* genome version 3.1 using proseq2.0 pipeline [57]. Regulatory elements were predicted with the vector machine learning tool dREG [15]. Two biological and one technical replicate libraries were prepared and paired or single end sequenced, providing a total of 56,781,051 20-h and 28,430,031 12-h mapped reads, excluding ribosomal RNAs.

For ChIP-seq library preparation, 50 to 100 million nuclei were spun at 4000 g for 5 min at 4 °C. Nuclei were resuspended in 1 ml FA buffer (50 mM HEPES/KPH pH 7.5, 1 mM EDTA, 1% Triton X-100, 0.1% sodium deoxycholate, 150 mM NaCl, 0.1% sarkosyl, and protease and phosphatase inhibitors). The resuspended nuclei were then sonicated at 4 °C for 15 min on high, cycle of 30 s on and 30 s off, to obtain an extract with fragmented chromatin. Extracts were brought up to 440 µL with FA buffer with protease and phosphatase inhibitors. Between 1 to 2 mg of extract and 4 µg of antibody were used per ChIP. Prior to the addition of antibody, 5% of the extract was taken for input. Mouse monoclonal antibody against RNA polymerase II CTD-repeat YSPTSPS (8WG16; abcam ab817mod) was used for ChIP. The mixture was incubated rotating at 4 °C overnight. 40 µL of protein G sepharose bead slurry (GE Healthcare) per ChIP sample was washed three times with 1 mL FA buffer, added 40 µL bead slurry to each ChIP sample and rotated at 4 °C for 2 h. Meanwhile, 200 µL ChIP Elution Buffer (1% SDS, 250 mM NaCl, 10 mM Tris pH 8.0, 1 mM EDTA) and 2 µL 10 mg/µL RNase A were added to inputs and incubated at room temperature. Beads were washed at room temperature by adding 1 mL of each of the following buffers and collecting beads by spinning for 1 min at 2500 g: two times FA buffer for 5 min, one time FA-1 M NaCl for 5 min, one time FA-500 mM NaCl for 10 min, one time TEL buffer (0.25 M LiCl, 1% NP-40, 1% sodium deoxycholate, 1 mM EDTA, 10 mM Tris-HCl, pH 8.0) for 10 min, two times TE for 5 min. Proteinase K was added to both inputs and ChIPs and incubated in a 50 °C heat block for an hour. Inputs and ChIPs were allowed to reverse crosslink overnight in a 65 °C water bath. DNA was ligated to Illumina or home-made multiplexed adapters and amplified by PCR. Using a thin 1.5% agarose gel, DNA fragments between 300 and 600 bp were purified using the Qiagen Gel Extraction kit. Qubit fluorometer was used to measure DNA concentration. Single-end sequencing was performed for the ChIP-seq and input DNA at the New York

University Center for Genomics and Systems Biology high-throughput sequencing facility. We combined replicates and aligned 50 bp single end reads to the *S. purpuratus* genome version 3.1 linear scaffolds using Bowtie 2 version 2.2.3 [58] with default parameters. A total of 13,762,893 ChIP and 26,476,643 input mapped reads were obtained. Mapped reads from ChIP and input were used to call peaks and coverage per base using MACS version 1.4.2 [59] with default parameters.

### Computational analysis of PRO-, ChIP-, and ATAC-seq peak calls and machine learning, enhancer activity prediction

Signal at PRO-, ChIP-, and ATAC-seq peak calls was quantified using the R package bigWig [60]. ATAC and PRO-seq reads of 12 and 20 h embryos were normalized to reads per million per base. For ATAC-seq peak calls, any overlapping peaks were merged prior to analysis. Density plots used R lift posted in StackOverflow [61]. Overlaps among PRO-, ChIP-, and ATAC-seq peak calls were analyzed and illustrated with ChIPpeakAnno [62] using default parameters. Promoters are defined as the 200 bp region centered at the 5' end of transcript based gene models, which are a better approximations than GLEAN models [36]. For all data sets, reads from different replicates were merged into single bigwig files and reads computed at peak calls and dREG predictions using the bigWig interface [60].

Using bedtools [63], the intersections between dREG predictions and CRMs were merged, to correct for CRM overlaps, and then extended 50 bp, to compute the pause associated PRO-seq reads oftentimes extending beyond the raw dREG prediction. The total number of 3' end reads in the plus and minus strand and the summit for each TRE prediction was estimated with the sum and max parameters of the bigWig query function. Similar analysis was performed for the reads per base for the intersection with ATAC- and Pol II ChIP peaks, without the 50 bp extension. Graphics were elaborated with ggplot and tidyverse [64].

The package caret was used for the optimization, test and evaluation of classification and regression models [65]. Logistic classification and linear regression models were fitted and tested by 5 fold cross-validation with stratified sampling repeated 200 times. The package precrec [66] was used to generate ROCs and PRCs.

### Abbreviations

ATAC-seq: Assay for Transposase-Accessible Chromatin using sequencing; AUPRC: Area under the Precision-Recall Curve; AUROC: Area under the Receiver Operating Characteristic Curve; BAC: Bacterial Artificial Chromosome; ChIP-seq: Chromatin Immunoprecipitation followed by sequencing; CRM: *cis*-regulatory module; dREG: Discriminative regulatory-element detection from GRO-seq; GRN: Gene regulatory network; MACS: Model-based Analysis for ChIP-seq; Pol II: RNA polymerase II; PRC: Precision-Recall Curve; PRO-seq: Precision nuclear run-on sequencing; ROC: Receiver Operating

Characteristic Curve; TRE: Transcriptional regulatory element; TSS: Transcription start site

## Supplementary Information

The online version contains supplementary material available at <https://doi.org/10.1186/s12864-021-07936-0>.

### Additional file 1.

**Additional file 2: Supplementary Table 1.** Genomic locations, genomic signals and reporter activities of the 389 CRMs.

**Additional file 3: Fig. S1.** Promoter and CRM PRO-, ATAC- and ChIP-seq analysis.

**Additional file 4: Fig. S2.** PRO-, Pol II ChIP- and ATAC-seq at *onecut*, *gcm*, *gatae* and *delta*. A, *onecut*, the entire region was scanned for enhancer activity by overlapping reporter constructs averaging 2.23 Kb [40]. Similar snapshots are taken for other regulatory genes whose regulatory elements were primarily selected based on evolutionary sequence conservation rather than an unbiased tiling scan.

**Additional file 5: Fig. S3.** The enhancer activity of promoter-overlapping CRMs is independent of their orientation. A, the concurrent orientation of the promoter in the GFP reporter construct and the promoter of promoter-overlapping CRMs could in principle result in transcripts reaching to the coding region of the reporter that could confound CRM driven transcription (red dashed line) with enhancer activity (black dotted line). In both cases the reporter enhancer activity of CRMs containing endogenous promoters should be diminished due to enhancer sharing between both promoters. Correlation of Pol II accumulation at endogenous promoters (purple ovals) and reporter expression is expected for CRMs that contain necessary enhancers and endogenous promoters. B, the difference of expression between CRMs in concurrent and divergent reporter construct orientation is not significant (ns) in 12 and 24 h embryos, Wilcoxon test  $p$ -values of 0.67 and 0.14, respectively.

**Additional file 6: Fig. S4.** Evaluation of models for CRMs overlapping and not overlapping promoters. A, 12 h embryo and, B, 20 h embryo models trained and tested with CRMs not overlapping promoters. C, 12 h embryo and, D, 20 h embryo models trained and tested with CRMs overlapping promoters.

**Additional file 7: Fig. S5.** Quantitative prediction of enhancer activity from ATAC and PRO-seq data. Plot of the hold-out predicted and actual reporter expression of linear regression models using ATAC and PRO-seq signal in 12 h and 20 h stages. Violin/Box-plots of  $R^2$  values, with the average indicated underneath.

**Additional file 8: Fig. S6.** Summary 12 to 20 h mRNA expression changes of regulatory genes. The fold change in the mRNA expression levels quantified at high resolution for 31 of the 37 genes used in this study [33].

### Acknowledgements

We would like to thank Jongmin Nam for providing the datasets associated with his CRM quantitative analysis, Charles A. Ettensohn for facilitating the contribution of Tanvi Shashikant while working in his lab, the Bioinformatics High Performance Computing personnel at Cornell University for the technical assistance received, all members of the Danko lab for their help and Professor Zhong Wang in particular for his assistance during the early phases of the computational analysis.

### Authors' contributions

Zihe Wang, César Arenas-Mena, Sofija Miljovska, Edward J. Rice, Justin Gurges, Tanvi Shashikant, Sevinç Ercan, Charles G. Danko. CA-M designed and optimized the nuclear extraction protocols, performed the density gradient nuclear preps, various PRO-seq experiments, the ATAC-seq replicates of 12 h embryos, the genomic mapping of ATAC and PRO-seq reads and subsequent processing, the manual curation of genomic profiles, contributed to the design and executed the machine learning analysis and wrote the manuscript and Figs. SM performed the Pol II ChIP-seq experiment and the ATAC-seq replicates in 20 h embryos. EJ performed the first PRO-seq replicate in 20 h embryos and assisted in the elaboration of 12 and 20 h embryo replicates.

JG participated in the optimization of early nuclear extraction protocols and obtained the nuclear preps for the first round of 20 h ATAC-seq replicates and the ChIP-seq nuclear preps. TS performed the first round of ATAC-seq genomic mapping and ChIP-seq and ATAC-seq peak call analysis. ZW identified the concurrent or divergent orientation of reporter constructs and compared their expression. SE designed and supervised the ATAC-seq experiments in 20 h embryos and Pol II ChIP-seq experiments. CGD supervised and analyzed the first PRO-seq replicate in 20 h embryos, contributed to the conceptual design of the machine learning model approach, supervised all computational analysis and statistical methods, and supervised the illustration and writing of the manuscript. All authors read and approved the final manuscript.

### Funding

This project was funded by NASA award 80NSSC18K1090 to Cornell University and CSI subaward 84502-11114.

### Availability of data and materials

The datasets generated and analyzed during the current study are available at NCBI GEO under accession number GSE160463 [44]. <https://www.ncbi.nlm.nih.gov/geo/query/acc.cgi?acc=GSE160463>

### Declarations

#### Ethics approval and consent to participate

Not Applicable.

#### Consent for publication

All authors read and approved the final manuscript.

#### Competing interests

The authors declare that they have no competing interests.

#### Author details

<sup>1</sup>College of Staten Island, The City University of New York (CUNY), Staten Island, NY 10314, USA. <sup>2</sup>Programs in Biology and Biochemistry, The Graduate Center, CUNY, New York, NY 10016, USA. <sup>3</sup>Department of Biology, New York University, New York, NY 10003, USA. <sup>4</sup>Baker Institute for Animal Health, College of Veterinary Medicine, Cornell University, Ithaca, NY 14853, USA. <sup>5</sup>Department of Biological Sciences, Carnegie Mellon University, Pittsburgh, PA, USA. <sup>6</sup>Center for Genomics and Systems Biology, New York University, New York, NY 10003, USA. <sup>7</sup>Department of Biomedical Sciences, College of Veterinary Medicine, Cornell University, Ithaca, NY 14853, USA.

Received: 15 March 2021 Accepted: 28 June 2021

Published online: 19 October 2021

### References

- Andersson R, Sandelin A, Danko CG. A unified architecture of transcriptional regulatory elements. *Trends Genet.* 2015;31(8):426–33 <https://doi.org/10.1016/j.tig.2015.05.007>.
- Arenas-Mena C. The origins of developmental gene regulation. *Evol Dev.* 2017;19(2):96–107 <https://doi.org/10.1111/ede.12217>.
- Britten RJ, Davidson EH. Gene regulation for higher cells: a theory. *Science.* 1969;165(663):349–57 <https://doi.org/10.1126/science.165.3891.349>.
- Peter IS, Davidson EH. Genomic control process: development and evolution. San Diego: Academic Press; 2015. p. 460.
- Haberle V, Stark A. Eukaryotic core promoters and the functional basis of transcription initiation. *Nat Rev Mol Cell Biol.* 2018;19(10):621–37 <https://doi.org/10.1038/s41580-018-0028-8>.
- Andersson R, Sandelin A. Determinants of enhancer and promoter activities of regulatory elements. *Nat Rev Genet.* 2020;21(2):71–87 <https://doi.org/10.1038/s41576-019-0173-8>.
- Haberle V, Lenhard B. Promoter architectures and developmental gene regulation. *Semin Cell Dev Biol.* 2016;57:11–23 <https://doi.org/10.1016/j.semcdb.2016.01.014>.
- Davidson EH, Levine MS. Properties of developmental gene regulatory networks. *Proc Natl Acad Sci.* 2008;105(51):20063–6 <https://doi.org/10.1073/pnas.0806007105>.

9. Gasperini M, Tome JM, Shendure J. Towards a comprehensive catalogue of validated and target-linked human enhancers. *Nat Rev Genet.* 2020;21(5):292–310 <https://doi.org/10.1038/s41576-019-0209-0>.
10. Klein JC, Agarwal V, Inoue F, Keith A, Martin B, Kircher M, et al. A systematic evaluation of the design and context dependencies of massively parallel reporter assays. *Nat Methods.* 2020;17(11):1083–91 <https://doi.org/10.1038/s41592-020-0965-y>.
11. Sethi A, Gu M, Gumusgoz E, Chan L, Yan K-K, Rozowsky J, et al. Supervised enhancer prediction with epigenetic pattern recognition and targeted validation. *Nat Methods.* 2020;17(8):807–14 <https://doi.org/10.1038/s41592-020-0907-8>.
12. Ernst J, Kheradpour P, Mikkelson TS, Shores N, Ward LD, Epstein CB, et al. Mapping and analysis of chromatin state dynamics in nine human cell types. *Nature.* 2011;473(7345):43–9 <https://doi.org/10.1038/nature09906>.
13. Monti R, Barozzi I, Osterwalder M, Lee E, Kato M, Garvin TH, et al. Limb-enhancer genie: an accessible resource of accurate enhancer predictions in the developing limb. Ioshikhes I, editor. *PLoS Comput Biol.* 2017;13(8):e1005720. <https://doi.org/10.1371/journal.pcbi.1005720>
14. Bozek M, Gompel N. Developmental transcriptional enhancers: a subtle interplay between accessibility and activity. *BioEssays.* 2020;42(4):1900188 <https://doi.org/10.1002/bies.201900188>.
15. Wang Z, Chu T, Choate LA, Danko CG. Identification of regulatory elements from nascent transcription using dREG. *Genome Res.* 2019;29(2):293–303 <https://doi.org/10.1101/gr.238279.118>.
16. Mikhaylichenko O, Bondarenko V, Harnett D, Schor IE, Males M, Viales RR, et al. The degree of enhancer or promoter activity is reflected by the levels and directionality of eRNA transcription. *Genes Dev.* 2018;32(1):42–57 <https://doi.org/10.1101/gad.308619.117>.
17. Chu T, Rice EJ, Booth GT, Salamanca HH, Wang Z, Core LJ, et al. Chromatin run-on and sequencing maps the transcriptional regulatory landscape of glioblastoma multiforme. *Nat Genet.* 2018;50(11):1553–64 <https://doi.org/10.1038/s41588-018-0244-3>.
18. Tippens ND, Liang J, Leung AK-Y, Wierbowski SD, Ozer A, Booth JG, et al. Transcription imparts architecture, function and logic to enhancer units. *Nat Genet.* 2020;52(10):1067–75 <https://doi.org/10.1038/s41588-020-0686-2>.
19. Core LJ, Martins AL, Danko CG, Waters CT, Siepel A, Lis JT. Analysis of nascent RNA identifies a unified architecture of initiation regions at mammalian promoters and enhancers. *Nat Genet.* 2014;46(12):1311–20 <https://doi.org/10.1038/ng.3142>.
20. Kwak H, Fuda NJ, Core LJ, Lis JT. Precise maps of RNA polymerase reveal how promoters direct initiation and pausing. *Science.* 2013;339(6122):950–3 <https://doi.org/10.1126/science.1229386>.
21. Li E, Cui M, Peter IS, Davidson EH. Encoding regulatory state boundaries in the pregastrular oral ectoderm of the sea urchin embryo. *Proc Natl Acad Sci.* 2014;111(10):E906–13 <https://doi.org/10.1073/pnas.1323105111>.
22. Oliveri P, Tu Q, Davidson EH. Global regulatory logic for specification of an embryonic cell lineage. *Proc Natl Acad Sci.* 2008;105(16):5955–62 <https://doi.org/10.1073/pnas.0711220105>.
23. Peter IS, Davidson EH. A gene regulatory network controlling the embryonic specification of endoderm. *Nature.* 2011;474(7353):635–9 <https://doi.org/10.1038/nature10100>.
24. Cui M, Vielmas E, Davidson EH, Peter IS. Sequential response to multiple developmental network circuits encoded in an Intronic cis-regulatory module of sea urchin *hox11/13b*. *Cell Rep.* 2017;19(2):364–74 <https://doi.org/10.1016/j.celrep.2017.03.039>.
25. Hajdu M, Calle J, Puno A, Haruna A, Arenas-Mena C. Transcriptional and post-transcriptional regulation of histone variant *H2A.Z* during sea urchin development. *Develop Growth Differ.* 2016;9(3):231–43. <https://doi.org/10.1111/dgd.12329>
26. Revilla-i-Domingo R, Oliveri P, Davidson EH. A missing link in the sea urchin embryo gene regulatory network: *hesC* and the double-negative specification of micromeres. *Proc Natl Acad Sci.* 2007;104(30):12383–8 <https://doi.org/10.1073/pnas.0705324104>.
27. Flytzanis CN, McMahon AP, Hough-Evans BR, Katula KS, Britten RJ, Davidson EH. Persistence and integration of cloned DNA in postembryonic sea urchins. *Dev Biol.* 1985;108(2):431–42 [https://doi.org/10.1016/0012-1606\(85\)90046-6](https://doi.org/10.1016/0012-1606(85)90046-6).
28. McMahon AP, Flytzanis CN, Hough-Evans BR, Katula KS, Britten RJ, Davidson EH. Introduction of cloned DNA into sea urchin egg cytoplasm: replication and persistence during embryogenesis. *Dev Biol.* 1985;108(2):420–30 [https://doi.org/10.1016/0012-1606\(85\)90045-4](https://doi.org/10.1016/0012-1606(85)90045-4).
29. Harmston N, Baresic A, Lenhard B. The mystery of extreme non-coding conservation. *Philos Trans R Soc Lond Ser B Biol Sci.* 2013;368(1632):20130021 <https://doi.org/10.1098/rstb.2013.0021>.
30. Villar D, Berthelot C, Aldridge S, Rayner TF, Lukk M, Pignatelli M, et al. Enhancer evolution across 20 mammalian species. *Cell.* 2015;160(3):554–66 <https://doi.org/10.1016/j.cell.2015.01.006>.
31. Shashikant T, Khor JM, Etensohn CA. Global analysis of primary mesenchyme cell cis-regulatory modules by chromatin accessibility profiling. *BMC Genomics.* 2018;19:1. <https://doi.org/10.1186/s12864-018-4542-z>
32. Nam J, Davidson EH. Barcoded DNA-tag reporters for multiplex cis-regulatory analysis. *PLoS One.* 2012;7(4):e35934 <https://doi.org/10.1371/journal.pone.0035934>.
33. Nam J, Dong P, Tarpipe R, Istrail S, Davidson EH. Functional cis-regulatory genomics for systems biology. *Proc Natl Acad Sci.* 2010;107(8):3930–5 <https://doi.org/10.1073/pnas.1000147107>.
34. Buenostro JD, Giresi PG, Zaba LC, Chang HY, Greenleaf WJ. Transposition of native chromatin for fast and sensitive epigenomic profiling of open chromatin, DNA-binding proteins and nucleosome position. *Nat Methods.* 2013;10(12):1213–8 <https://doi.org/10.1038/nmeth.2688>.
35. De Santa F, Barozzi I, Mietton F, Ghisletti S, Polletti S, Tusi BK, et al. A large fraction of extragenic RNA pol II transcription sites overlap enhancers. Mattick JS, editor. *PLoS Biol.* 2010;8(5):e1000384. <https://doi.org/10.1371/journal.pbio.1000384>
36. Tu Q, Cameron RA, Davidson EH. Quantitative developmental transcriptomes of the sea urchin *Strongylocentrotus purpuratus*. *Dev Biol.* 2014;385(2):160–7 <https://doi.org/10.1016/j.ydbio.2013.11.019>.
37. Malik A, Gildor T, Sher N, Layous M, Ben-Tabou de-Leon S. parallel embryonic transcriptional programs evolve under distinct constraints and may enable morphological conservation amidst adaptation. *Dev Biol.* 2017;430(1):202–13 <https://doi.org/10.1016/j.ydbio.2017.07.019>.
38. Arenas-Mena C, Cameron RA, Davidson EH. Hindgut specification and cell-adhesion functions of *Sphox11/13b* in the endoderm of the sea urchin embryo. *Develop Growth Differ.* 2006;48(7):463–72 <https://doi.org/10.1111/j.1440-169X.2006.00883.x>.
39. Chambers M, Turki-Judeh W, Kim MW, Chen K, Gallaher SD, Courey AJ. Mechanisms of Groucho-mediated repression revealed by genome-wide analysis of Groucho binding and activity. *BMC Genomics.* 2017;18(1):215 <https://doi.org/10.1186/s12864-017-3589-6>.
40. Barsi JC, Davidson EH. cis-regulatory control of the initial neurogenic pattern of *onecut* gene expression in the sea urchin embryo. *Dev Biol.* 2016;409(1):310–8 <https://doi.org/10.1016/j.ydbio.2015.10.021>.
41. Ransick A, Davidson EH. cis-regulatory processing of notch signaling input to the sea urchin glial cells missing gene during mesoderm specification. *Dev Biol.* 2006;297(2):587–602 <https://doi.org/10.1016/j.ydbio.2006.05.037>.
42. Revilla-i-Domingo R, Minokawa T, Davidson EH. R11: a cis-regulatory node of the sea urchin embryo gene network that controls early expression of *SpDelta* in micromeres. *Dev Biol.* 2004;274(2):438–51 <https://doi.org/10.1016/j.ydbio.2004.07.008>.
43. Lee PY, Nam J, Davidson EH. Exclusive developmental functions of gate cis-regulatory modules in the *Strongylocentrotus purpuratus* embryo. *Dev Biol.* 2007;307(2):434–45 <https://doi.org/10.1016/j.ydbio.2007.05.005>.
44. NCBI Gene Expression Omnibus. <https://www.ncbi.nlm.nih.gov/geo/query/acc.cgi?acc=GSE160463>. Accessed 23 Aug 2021.
45. Davidson Lab Gene Regulatory Networks. [https://wiki.echinobase.org/echinowiki/index.php/Davidson\\_Lab\\_Gene\\_Regulatory\\_Networks#Endomesoderm\\_Network\\_Views](https://wiki.echinobase.org/echinowiki/index.php/Davidson_Lab_Gene_Regulatory_Networks#Endomesoderm_Network_Views). Accessed 23 Aug 2021.
46. Saito T, Rehmsmeier M. The precision-recall plot is more informative than the ROC plot when evaluating binary classifiers on imbalanced datasets. *PLoS One.* 2015;10(3):e0118432 <https://doi.org/10.1371/journal.pone.0118432>.
47. Quintero-Cadena P, Sternberg PW. Enhancer sharing promotes neighborhoods of transcriptional regulation across eukaryotes. *G3.* 2016;6(12):4167. <https://doi.org/10.1534/g3.116.036228>
48. Engreitz JM, Haines JE, Perez EM, Munson G, Chen J, Kane M, et al. Local regulation of gene expression by lncRNA promoters, transcription and splicing. *Nature.* 2016;539(7629):452–5 <https://doi.org/10.1038/nature20149>.
49. Zabidi MA, Arnold CD, Schemhuber K, Pagani M, Rath M, Frank O, et al. Enhancer-core-promoter specificity separates developmental and housekeeping gene regulation. *Nature.* 2014;518(7540):556–9 <https://doi.org/10.1038/nature13994>.

50. Barolo S, Posakony JW. Three habits of highly effective signaling pathways: principles of transcriptional control by developmental cell signaling. *Genes Dev.* 2002;16(10):1167–81 <https://doi.org/10.1101/gad.976502>.
51. Zabidi MA, Stark A. Regulatory enhancer–Core-promoter communication via transcription factors and cofactors. *Trends Genet.* 2016;32(12):801–14 <https://doi.org/10.1016/j.tig.2016.10.003>.
52. Davidson EH, Rast JP, Oliveri P, Ransick A, Calestani C, Yuh C-H, et al. A provisional regulatory gene network for specification of Endomesoderm in the sea urchin embryo. *Dev Biol.* 2002;246(1):162–90 <https://doi.org/10.1006/dbio.2002.0635>.
53. Jonkers I, Lis JT. Getting up to speed with transcription elongation by RNA polymerase II. *Nat Rev Mol Cell Biol.* 2015;16(3):167–77 <https://doi.org/10.1038/nrm3953>.
54. Boettiger AN, Levine M. Synchronous and stochastic patterns of gene activation in the *Drosophila* embryo. *Science.* 2009;325(5939):471–3 <https://doi.org/10.1126/science.1173976>.
55. Poglitsch M, Katholnig K, Säemann MD, Weichhart T. Rapid isolation of nuclei from living immune cells by a single centrifugation through a multifunctional lysis gradient. *J Immunol Methods.* 2011;373(1–2):167–73 <https://doi.org/10.1016/j.jim.2011.08.012>.
56. ENCODE ATAC-seq pipeline. <https://github.com/ENCODE-DCC/atac-seq-pipeline>. Accessed 23 Aug 2021.
57. Danko-Lab. proseq2.0. <https://github.com/Danko-Lab/proseq2.0>. Accessed 23 Aug 2021.
58. Langmead B, Salzberg SL. Fast gapped-read alignment with bowtie 2. *Nat Methods.* 2012;9(4):357–9 <https://doi.org/10.1038/nmeth.1923>.
59. Zhang Y, Liu T, Meyer CA, Eeckhoute J, Johnson DS, Bernstein BE, et al. Model-based analysis of ChIP-Seq (MACS). *Genome Biol.* 2008;9(9):R137 <https://doi.org/10.1186/gb-2008-9-9-r137>.
60. AndreImartins bigWig. <https://github.com/andreImartins/bigWig>. Accessed 23 Aug 2021.
61. Stackoverflow. R Scatter Plot: symbol color represents number of overlapping points. <http://stackoverflow.com/questions/17093935/r-scatter-plot-symbol-color-represents-number-of-overlapping-points>. Accessed 23 Aug 2021.
62. Zhu LJ, Gazin C, Lawson ND, Pagès H, Lin SM, Lapointe DS, et al. ChIPpeakAnno: a Bioconductor package to annotate ChIP-seq and ChIP-chip data. *BMC Bioinformatics.* 2010;11(1):237 <https://doi.org/10.1186/1471-2105-11-237>.
63. Quinlan AR, Hall IM. BEDTools: a flexible suite of utilities for comparing genomic features. *Bioinformatics.* 2010;26(6):841–2 <https://doi.org/10.1093/bioinformatics/btq033>.
64. Tidyverse. <https://www.tidyverse.org/>. Accessed 23 Aug 2021.
65. Kuhn M. Building predictive models in R using the caret Package. *J Stat Softw.* 2008;28(5) Available from: <http://www.jstatsoft.org/v28/i05/>. [cited 2020 Sep 17].
66. Saito T, Rehmsmeier M. PreRec: fast and accurate precision–recall and ROC curve calculations in R. *Bioinformatics.* 2017;33(1):145–7 <https://doi.org/10.1093/bioinformatics/btw570>.

## Publisher's Note

Springer Nature remains neutral with regard to jurisdictional claims in published maps and institutional affiliations.

**Ready to submit your research? Choose BMC and benefit from:**

- fast, convenient online submission
- thorough peer review by experienced researchers in your field
- rapid publication on acceptance
- support for research data, including large and complex data types
- gold Open Access which fosters wider collaboration and increased citations
- maximum visibility for your research: over 100M website views per year

**At BMC, research is always in progress.**

Learn more [biomedcentral.com/submissions](https://biomedcentral.com/submissions)

